ARMY RESEARCH LABORATORY

Doppler Signature Measurements of an Mi-24 Hind-D Helicopter at 92 GHz

by Ronald J. Wellman and Jerry L. Silvious

ARL-TR-1637

July 1998

19980820 078

Approved for public release; distribution unlimited.

DTIC QUALITY INSPECTED 1

Army Research Laboratory

Adelphi, MD 20783-1197

Doppler Signature Measurements of an Mi-24 Hind-D Helicopter at 92 GHz

Ronald J. Wellman and Jerry L. Silvious
Sensors and Electron Devices Directorate

Abstract

This report describes millimeter wave Doppler signature measurements made on a hovering Mi-24 Hind-D helicopter. The measurement system, a CW sensor operating at 92 GHz, is described in detail. The recording system consisted of a high speed A/D board installed in a dual Pentium computer running Windows NT. The report presents the results of the Doppler analysis of the data. The signatures created by the rotating blades of the jet turbines known as jet engine modulation (JEM) lines and the Doppler signature components created by the many moving parts of the main and tail rotor assemblies are discussed in detail and a comparison to the theoretical values is presented.

Contents

Figures

Tables

1. Introduction

Sensor systems operating in the millimeter wave (MMW) spectrum require precise signature information in order to detect and classify targets of interest. In general, these targets have both static and Doppler signatures that can vary drastically with orientation and depression angle, and thus make it difficult to identify individual target types. Airborne targets such as helicopters and airplanes exhibit very distinct Doppler signatures. These signatures consist of the jet engine modulation (JEM) lines caused by the rotating blades of the jet turbines and, for helicopters in particular, the Doppler signature components created by the many moving parts of the main and tail rotor assemblies. The purpose of this work was to measure the signature of a Hind-D helicopter at MMW frequencies so that algorithms for accurately identifying this particular helicopter could be developed. We describe the measurement system, calibration, and measurement procedures in section 2 of this report; discuss the measurement results in section 3; and present our conclusions in section 4.

2. Radar Description and Measurements

2.1   Description of the Doppler Measurement System

A block diagram of the system used to make the measurements is shown in figure 1. The system was designed around a 200-mW MMW source operating at 92 GHz. A directional coupler is used with an up-converter to combine some of this MMW power with a 3-GHz intermediate frequency (IF) signal to generate a 95-GHz signal at about 0 dBm. This signal is amplified by an MMW stable amplifier to +10 dBm and then passed through a low-pass filter to provide +7 dBm local oscillator (LO) power to

Figure 1. Block diagram of Doppler measurement system.

1
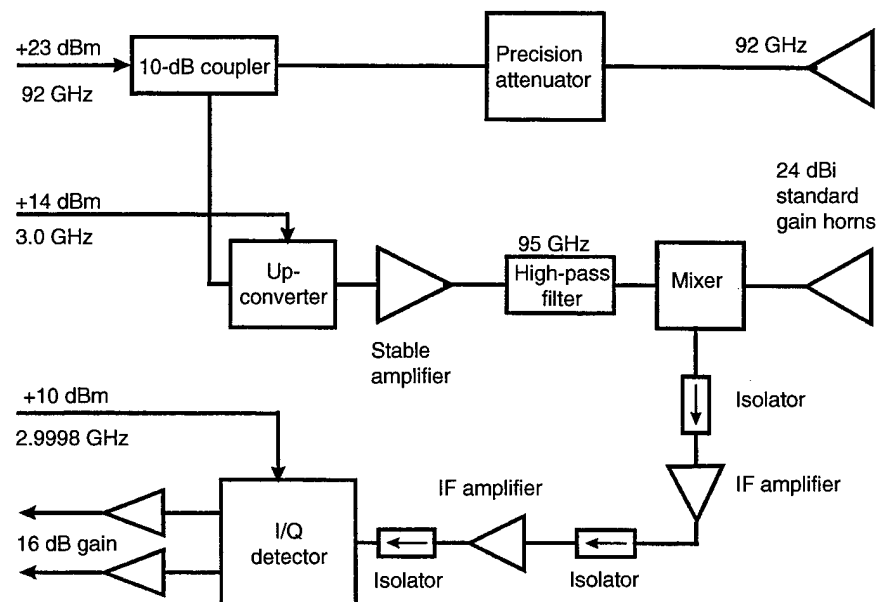
the balanced mixer. The remaining portion of the 92-GHz power continues through a precision attenuator and a 24-dBi standard gain horn used as the transmitter antenna. A matching horn is used for the receiver antenna, with both horns oriented for vertical polarization. The received power feeds a balanced mixer. The IF output from the mixer is amplified, isolated, and then injected into the rf port of a 3-GHz in-phase/quadrature (I/Q) detector. The LO power for the I/Q detector is supplied by a laboratory synthesizer operating at 2.9998 GHz. These two frequencies create an offset frequency that corresponds to system leakage and fixed clutter of 200 kHz. The maximum expected frequency created by the hovering helicopter is expected to be about 150 kHz. The outputs of the I/Q detector are amplified with two 16-dB gain amplifiers to match the dynamic range of the dual-channel analog-to-digital converters (A/Ds) that digitize the measured signal. The radar head is mounted on a computer controlled elevation-over-azimuth positioner that provides extremely accurate control of the radar pointing angle.

The data acquisition computer is a dual 133-MHz Pentium system that runs on Windows NT. The computer includes a general purpose interface bus (GPIB) control card and dual channel, 12-bit, 10-MHz high speed A/D card. The Labview Software package was chosen to control the sensor operation, pedestal motion, and data acquisition. Both the control card and the data acquisition board are supported by Labview. The A/D board is fully programmable and supports either single- or dual-channel operation at sample rates up to 10 MHz per channel. Sample rates from 1 to 10 MHz were used for the data acquisition. We decided to use only one channel of the I/Q detector so that a separate I/Q calibration would not be necessary. Because we were only interested in the spectrum, the measured data were calibrated by performing a fast Fourier transform (FFT) and referencing the output to the FFT of a calibration reflector. In this manner, the body line and any fixed clutter from the background occurred at 200 kHz, and the spectrum was centered about this line. The single channel was simply sampled at twice the highest frequency of interest and only one-half of the spectrum was retained for analysis. The 200-kHz offset frequency guaranteed that the complete spectrum would be contained in the upper half of the FFT. Data were acquired with sample rates of 1 MHz, 2 MHz, 5 MHz, and 10 MHz, with the primary data taken at the 1-MHz rate. The A/D card has the capability to store up to 1,048,576 samples of data at a time; this corresponds to a data acquisition sample window of 1.048 s at the 1-MHz rate. This combination provides a frequency resolution of about 1 Hz.

2.2   Doppler Calibration

The calibration technique used for these measurements was quite simple. Because we were interested only in the spectrum of the helicopter, an absolute calibration of the static radar cross section (RCS) of the helicopter was not required. This was fortunate because the system leakage and the static background clutter limited our ability to measure the absolute RCS from the body of the helicopter. We chose to calibrate the spectrum by comparing the measured RCS to that measured from a 28.4-dBsm trihedral at a range of 44.4 m. The range to the center of the helicopter was 105.5 m, which requires a range correction of 15 dB. The reference trihedral and the leakage signal were measured before each run by acquiring 1 million samples at a 1-MHz sample rate. These data were processed with a 1-million-point FFT to generate the reference and leakage level responses. The peak amplitude of the trihedral FFT established the 28.4-dBsm reference level, while the leakage signal determined the minimum detectable static RCS. The target aspect angle, reference level, and leakage level for each data run are shown in table 1. The peak cell location was always cell 209716, which corresponds to an offset frequency of 200 kHz. The variation in the peak amplitude measured from the reference reflector is due to the wind-induced movement of the reference reflector, which causes spreading of the FFT spectrum and a resulting drop in the peak amplitude. The leakage signal is caused by the combination of waveguide leakage and the 92-GHz signal passing through the stable amplifier and high-pass filter. The high-pass filter was originally designed to block 91 GHz and pass 95 GHz. At 92 GHz, we were operating on the edge of the pass band so that variations in temperature caused noticeable changes in the filter loss at 92 GHz. The combination of the filter leakage and waveguide leakage that had been coherently summed in the mixer created the observed variations in leakage. This leakage limited the minimum detectable stationary target RCS. At the target range of 105 m, the leakage signal corresponds to an equivalent RCS of about 20 dBsm. However, the stationary clutter illuminated by the antenna pattern, 11° in azimuth by 14° in elevation, limited the minimum detectable target body RCS to at least 30 dBsm or more.

Table 1. Measured reference and leakage levels for Doppler calibration.

File name	Target aspect angle (°)	Peak cell no.	Reference amplitude (dB)	Leakage amplitude (dB)
H000.1024.1MHz.002	24	209716	52	32.4
H045.1024.1MHz.002	69	209716	54.4	33.8
H090.1024.1MHz.002	114	209716	52.1	35.5
H135.1024.1MHz.002	159	209716	55.8	30.6
H180.1024.1MHz.002	204	209716	56.3	30.8
H225.1024.1MHz.002	249	209716	56.3	28.6
H270.1024.1MHz.002	294	209716	54.5	23.1
H315.1024.1MHz.002	339	209716	51.7	28.6
H360.1024.1MHz.002	0	209716	54.2	29.4

2.3 Doppler Measurement Procedures

The Mi-24 Hind-D helicopter used for these measurements had been modified so that the helicopter engines could be run from a remote location. For this reason, we could only simulate a hovering condition. To simulate hovering, the helicopter was chained to a concrete blast pad at Aberdeen Proving Ground (APG) and operated in a wheels-light condition at normal engine speeds. Figure 2 shows the helicopter secured on the blast pad. To change the measurement aspect angle, the helicopter was lifted with a crane, repositioned at the proper angle, and then resecured to the pad. The time required to reposition the helicopter and acquire the data at each position was approximately 4 hrs. The helicopter was positioned at previously designated locations marked at every 45°, but due to the location of the radar, the aspect angles were offset from the cardinal angles by 24°. A final data run was made with the helicopter positioned at a relative angle of 0° so that the head-on signature could be obtained. The actual measured aspect angles are in table 1. At each aspect angle, measurements were made for a fixed set of sample rates and radar pointing angles. These included a measurement of the reference reflector, system leakage, and target Doppler signature at 1-MHz, 2-MHz, 5-MHz, and 10-MHz sample rates, and a two-channel (I and Q) measurement of the rotating and stationary target with clutter at a 1-MHz sample rate. An additional measurement was made of the rotating target with a 1-MHz sample rate at 4° to the right and left of the center of the helicopter. This was done to maximize the signal level from the main and tail rotor blade tips. The data files were processed with a 1-million-point FFT and then calibrated with the FFT response for the calibration reflector. A comparison of the two-channel FFT for the rotating and stationary target at 0° aspect angle is shown in figure 3. This figure demonstrates some of the important characteristics of the helicopter's Doppler signature such as the JEM lines, indicated by the narrow spectral lines, and the main rotor hub Doppler signature, indicated by the wide pedestal surrounding the helicopter body line. These characteristics are discussed in detail in the next section.

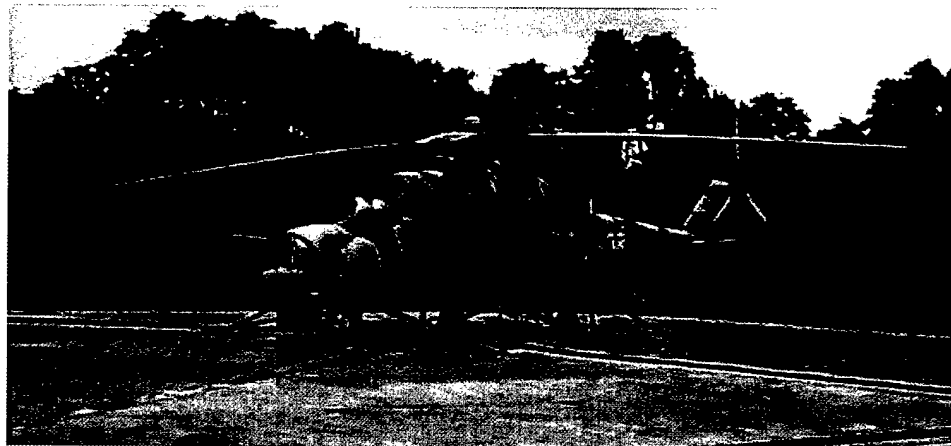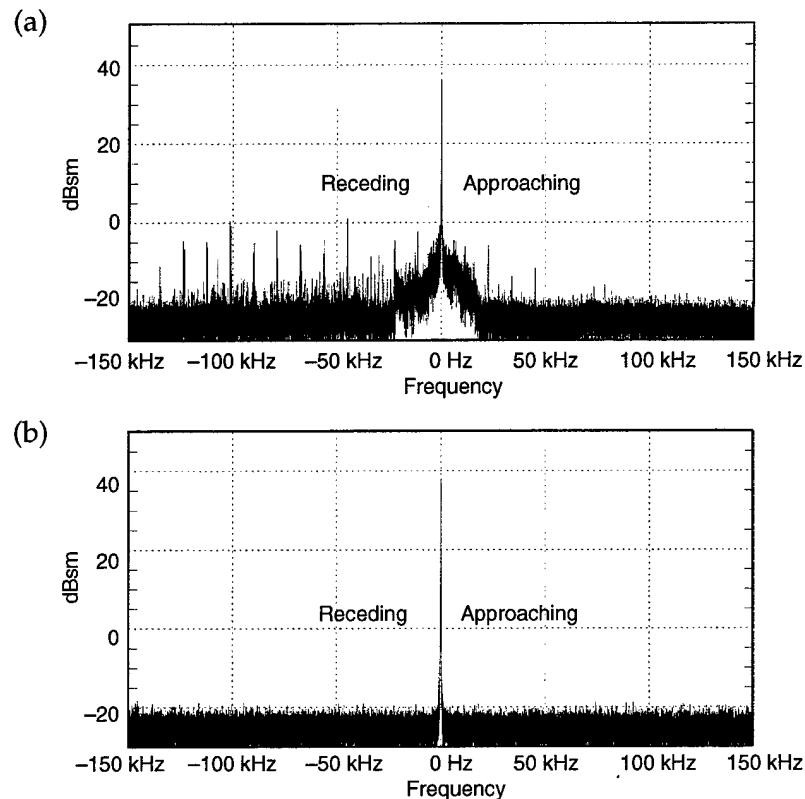**Figure 2. Hind-D helicopter configured for Doppler measurements.**

Figure 3. Comparison of (a) rotating and (b) stationary helicopter Doppler signatures measured at a 0° aspect angle.

(a)

(b)

3. Measurement Discussion

The Doppler spectrum of the helicopter is made up of two parts: the JEM lines, which are discrete spectral lines, and the Doppler spectrum, which is due to discrete moving parts such as the rotors and rotor hubs and tends to be distributed over a large range of frequencies. These components combine to create the overall Doppler spectrum of the helicopter. Because these two effects are quite different, we will discuss them separately.

3.1   Jet Engine Modulation Analysis

The JEM lines are due to the amplitude modulation of the backscattered signal created by the rotation of engine parts such as the compressor, turbine, or fan blades. These lines are visible only at aspect angles where the radiation from the radar can illuminate the rotation of these particular parts. The Hind-D helicopter has six possible sources for JEM lines: two engines with multiple compressors, two free turbines with multiple blades, one oil cooler, and an auxiliary power unit (APU) that also has a compressor. When we took measurements, the APU was in operation, but it may not be during normal flight. The JEM line frequency can be determined from the following formula:

$$F_J = RN/60 \; , \tag{1}$$

5

where F_J is the JEM frequency in hertz, R is the rotation rate in revolutions per minute (rpm), and N is the number of blades. The engine compressors and the free turbines have multiple sets of blades, and it is possible that more than one JEM line might be visible for certain aspect angles. The second set of lines would have a much lower amplitude than the first set of lines; so the measurement system sensitivity would determine whether multiple lines would be visible. Table 2 lists the different JEM sources, their respective rotation rates, the number of blades, and the calculated first harmonic JEM frequencies for all sets of blades. These frequencies are based on normal rotation-rate specifications for the Hind-D, and in general multiple harmonics of these frequencies will be visible.

The JEM line frequencies were most evident at certain aspect angles. The frequencies were determined by examining the Doppler spectrum primarily at these aspect angles although lines were visible at other aspect angles as well. The engine compressor and oil cooler JEM lines were most visible at the head-on or 0° aspect. The Doppler spectrum at the 0° aspect angle is shown in figure 4.

The display is the result of performing a 10^6-point FFT on the data and then plotting the frequency range of ±150 kHz about the zero frequency

Table 2. Hind-D helicopter JEM sources with calculated frequencies.

JEM source	Rotation rate (rpm)	No. of blades	Calculated frequency
Engine compressor	18,560	37	11,445
	18,560	43	13,301
	18,560	59	18,250
	18,560	67	20,725
Free turbine	15,000	51	12,750
	15,000	64	16,000
Oil cooler	6,000	19	1,900
APU	36,750	61	37,362

Figure 4. Doppler spectrum for Hind-D helicopter at 0° aspect angle.
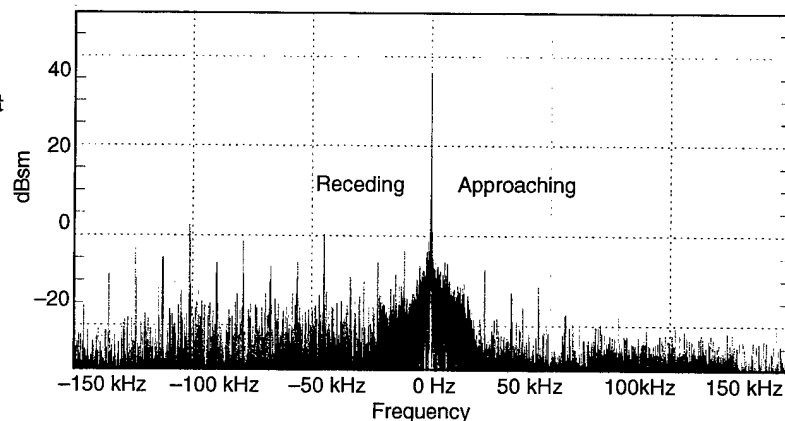
or body line of the helicopter. The JEM lines are indicated by the narrow spectral lines that are visible primarily on the receding Doppler part of the spectrum, although a few are evident on the approaching side as well. The engine compressor lines correspond to the narrow spectral lines that exceed −10 dBm spaced at 11-kHz intervals, while the oil cooler lines correspond to lines at about −15 dBm that are uniformly spaced at about 1.9-kHz intervals. To calculate the JEM frequencies for the engine compressors, the FFT array was filtered to find the larger amplitude lines, and then harmonic dependencies were determined. The oil cooler lines were more difficult to detect because the primary frequencies fall inside the hub Doppler region and were generally washed out. By determining the spacing between the smaller harmonically related lines and the few oil cooler lines that were large enough to see within the hub spectrum, we determined the oil cooler fundamental frequency. This same type of analysis was performed for the 114° and 249° aspect angles to determine the JEM frequencies for the two free turbines and the APU. These Doppler spectrums are shown in figures 5 and 6. The JEM lines are even more apparent when the data are processed in a slightly different manner.

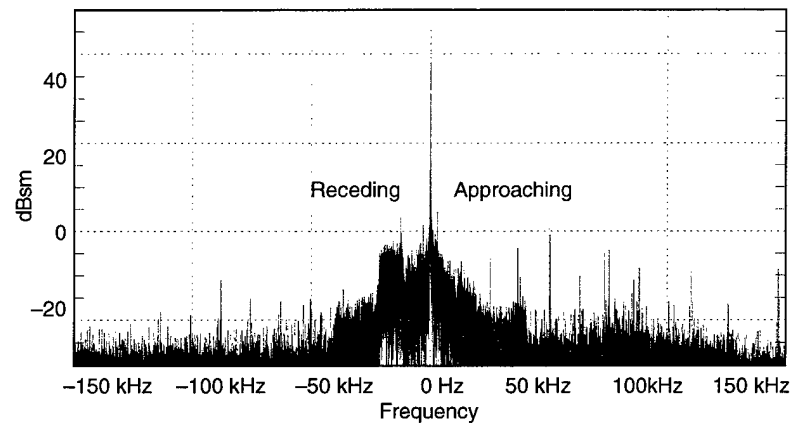**Figure 5. Doppler spectrum for Hind-D helicopter at 114° aspect angle.**

Figure 6. Doppler spectrum for Hind-D helicopter at 249° aspect angle.
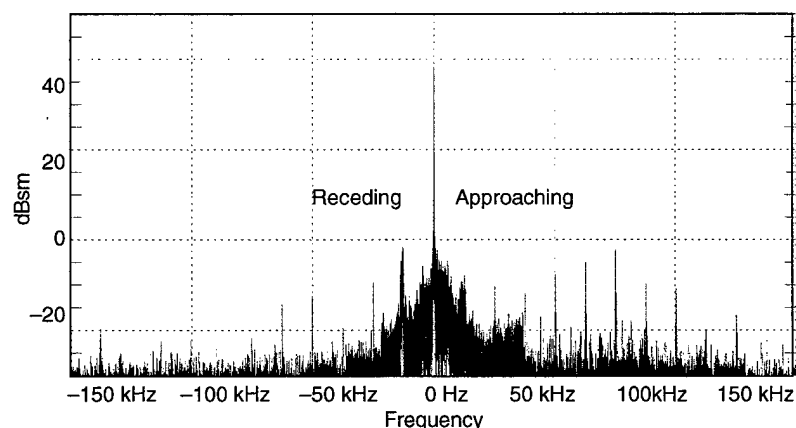

7

Figure 7 shows the Doppler-time spectrum measured at a 339° aspect angle. The figure was created by performing 512 2048-point FFTs with a 50 percent overlap, then plotting the frequency range from −150 kHz to +150 kHz versus the FFT number, with the FFT number being equivalent to time. In this figure, the JEM lines show up as time-independent lines at a fixed point in frequency space. In addition, the main rotor flashes and main hub Doppler spectrum are also visible. The measurements at the other aspect angles were examined to determine the range of aspect angles over which the various JEM lines were visible. The results of the JEM line analysis are in table 3. As indicated in the table, the agreement between the measured and calculated values for the JEM lines is good. All the measured frequencies are slightly lower than the calculated values, which probably indicates that the helicopter engines were being operated at slightly lower than normal engine rpm. Additionally, the two engines and the free turbines were operating at slightly different rpms as indicated by the slightly different JEM frequencies. As expected, the JEM lines were observed only at angles where the intake or exhaust ports of the various JEM sources were visible.

3.2 Doppler Analysis for Hind-D Helicopter

The true Doppler spectrum is that part of the signature that is caused by a Doppler shift of the incident radiation due to the motion of the scatterer perpendicular to the plane of propagation. The Doppler shift is given by the following simple formula:

$$F_D = (2v \cos\theta)/\lambda \ , \tag{2}$$

where F_D is the Doppler frequency, v is the component velocity, θ is the angle between the propagation vector and the velocity vector of the moving component, and λ is the wavelength. At 92 GHz, the wavelength λ is 3.26 mm. The major contributors to the Doppler frequency are the main rotor blades, main rotor hub assembly, and the tail rotor blades. The maximum velocity of the rotating components determines the maximum observed Doppler frequency, with the velocity given by

$$v = R_p d\pi/60 \ , \tag{3}$$

where R_p is the rotation rate in revolutions per minute and d is the diameter of the rotating component. The maximum expected Doppler frequencies for the main rotor blades, main rotor hub, and tail rotor blades are in table 4. In general, both positive and negative Doppler

Table 3. Measured JEM lines for hovering Hind-D helicopter.

JEM source	Rotation rate (rpm)	Calculated frequency	Measured frequency	Observed aspect angles
Engine 1 compressor	18,560	11,445	11,257	nose ± 45°
Engine 2 compressor	18,560	11,445	11,213	nose ± 45°
Oil cooler	6,000	1,900	1,875	nose ± 45°
Free turbine 1	15,000	12,750	12,579	90° ± 45°
Free turbine 2	15,000	12,750	12,543	270° ± 45°
APU	36,750	37,362	36,702	90° ± 45°

8

frequencies would be expected from these sources. Figures 8 and 9 show the main and tail rotor assemblies of the helicopter. The diameter of the main rotor hub shown in the table is measured to the point where the rotor blade front and back edges become parallel. This same dimension for the tail rotor would be about 1 m.

Figure 7. Doppler-time spectrum for Hind-D helicopter at 339° aspect angle.

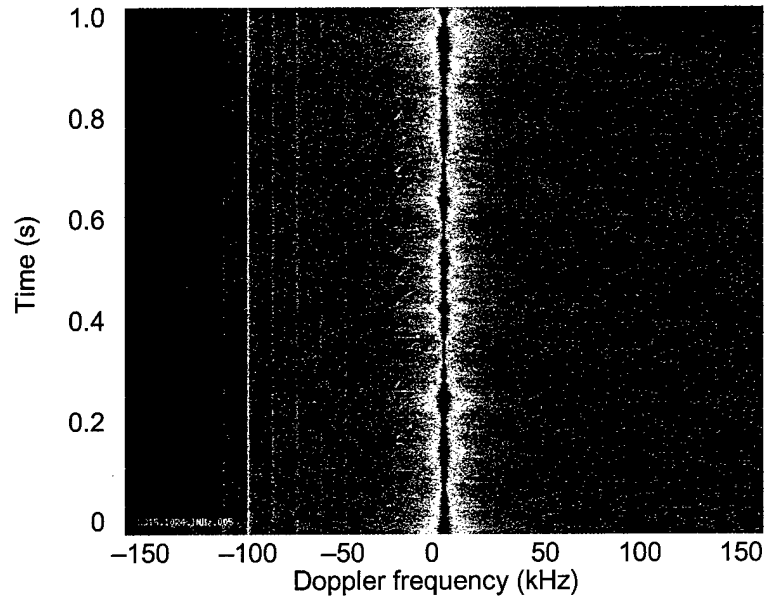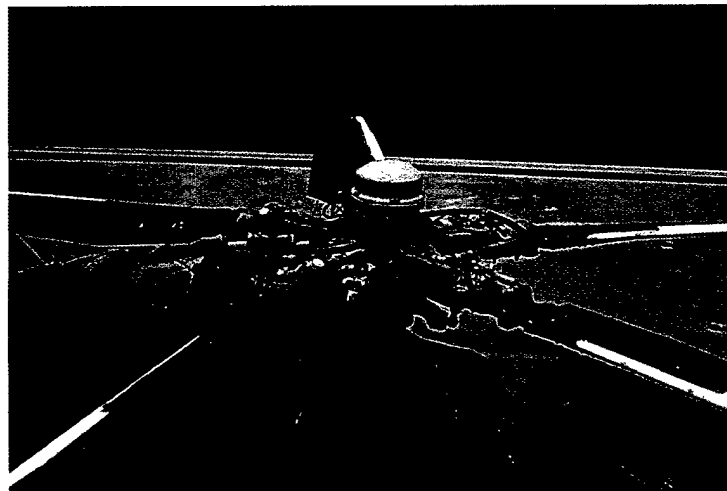**Table 4. Calculated Doppler frequencies for Hind-D helicopter.**

Doppler source	Rotation rate (rpm)	Diameter (m)	Maximum velocity (m/s)	Calculated Doppler frequency (kHz)
Main rotor blades	240	17.3	217.4	±133.4
Main rotor hub	240	3.0	37.7	±23.1
Tail rotor blades	1120	3.91	229.2	±140.6

Figure 8. Hind-D helicopter main rotor assembly.

9

As is apparent from figure 8, the main rotor hub assembly is much more complex than the tail rotor hub. Its many different potential scatterers at different radial positions create a complicated Doppler signature. The hub diameter constrains the entire Doppler signature to frequencies from –23 kHz to +23 kHz. (This is also shown in fig. 3.) A better representation of the Doppler signatures for the main rotor blades, main rotor hub, and tail rotor blades is shown in figure 10. The data have been processed in the same manner as in figure 7 except that the Doppler-time signature was measured at a 114° aspect angle and the radar was pointed 4° to the right of the center of the helicopter to maximize the tail rotor signature. This orientation corresponds to a 70° angle of incidence at the tail rotor.

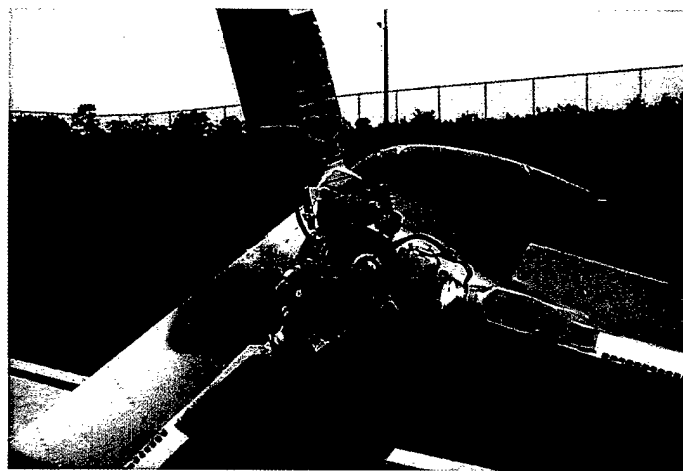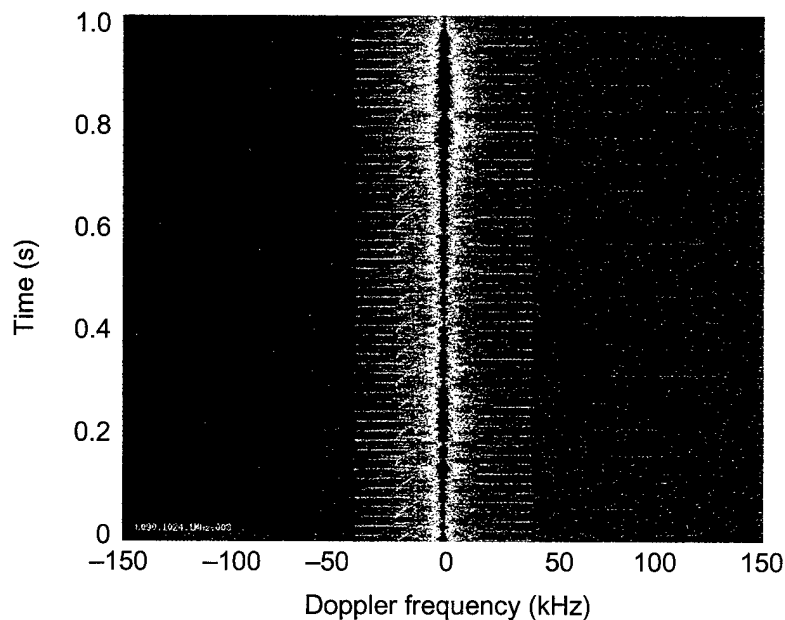**Figure 9. Hind-D helicopter tail rotor assembly.**

Figure 10. Doppler-time spectrum of Hind-D helicopter at 114° aspect angle.

10

At this orientation, the main rotor Doppler flashes were also optimized. The main rotor Doppler flash was visible at all aspect angles, but the signal level varied slightly over the different aspect angles. Only the forward edge, positive Doppler flash of the main rotor was visible in the Doppler spectrum. The geometry of the rotor blade—high RCS on the rounded front edge versus a low RCS from the sharp back edge—was responsible for this effect. On the other hand, the tail rotor Doppler flash exhibited both positive and negative Doppler frequencies, but the flash was only visible at the 114° and 249° aspect angles. This was caused by the measurement geometry, blades shielded by the fuselage for some aspect angles, and the low RCS of the tail rotor blades as viewed from the rear of the helicopter.

Figure 10 shows the main rotor, main rotor hub, and tail rotor Doppler frequencies that were determined along with the main and tail rotor rpm, which linearly affect the Doppler frequencies. The results are shown in table 5. The measured main rotor rotation rates were lower than expected at 227 rpm compared to 240 rpm; in fact, for the entire test this rotation rate varied from 225.5 to 228 rpm. The measured main hub and rotor Doppler frequencies are in excellent agreement with the calculated values when the correct rotation rate is used. As mentioned previously, only positive Doppler frequencies were seen from the main rotor flash, and for this aspect angle only negative Doppler frequencies were evident for the main rotor hub. However, for other aspect angles, some positive Doppler frequencies were included in the hub spectrum but, in general, there were more Doppler frequencies for the main rotor hub in the negative range. A more detailed measurement of only the main rotor hub's Doppler spectrum would help to identify the individual components of the hub that contribute to its signature. The tail rotor's Doppler frequency was measured at ±41 kHz compared to a calculated value of 133 kHz for a tail rotor rate of 1060 rpm. Both approaching and receding edges of the tail rotor were visible. The calculated value is for an angle of incidence of 0°, but the actual angle of incidence for this measurement was 70° and with the correction for $\cos\theta$, the expected Doppler frequency would be 45 kHz. The measured Doppler frequency corresponds to an incidence angle of 72°, which is well within the accuracy of our angle measurements. At the aspect angle of 249°, the measured tail rotor Doppler frequency was also in good agreement with the calculated values.

Table 5. Measured Doppler frequencies for Hind-D helicopter.

Doppler source	Rotation rate (rpm)	Diameter (m)	Calculated Doppler frequency (kHz)	Measured rotation rate (rpm)	Measured Doppler frequency (kHz)
Main rotor blades	240	17.3	±133.4	227	+127
Main rotor hub	240	3.0	±23.1	227	−22
Tail rotor blades	1120	3.91	±140.6	1060	±41

11

4. Conclusions

In this report, we have described in detail the Doppler signature measurements made on an Mi-24 Hind-D helicopter that was operating in a tethered simulated hover at APG during the summer of 1996. The measurements were made at a frequency of 92 GHz for aspect angles from 0° to 360° in 45° increments. The depression angle was approximately 0°. The helicopter was operated at engine speeds commensurate with normal flight. The measurement system was based on a 200-mW CW transmitter operating at 92 GHz with a coherent receiver operating at 95 GHz and both with vertically polarized standard gain horns. The received signal was digitized with a high speed A/D board that recorded 10^6 samples at sample rates from 1 MHz to 10 MHz.

We presented an analysis of the Doppler signatures that shows that the JEM lines generated by the engine compressors, free turbines, oil cooler, and APU were all detectable in the radar signature at aspect angles where the intake or exhaust of the sources was exposed. We have shown that the frequencies of these lines are proportional to the turbine rotation rate and number of turbine blades. We also have shown that only the primary set of turbine blades contributed to the Doppler signature. The analysis of the main rotor, main rotor hub, and tail rotor Doppler frequencies showed that

- the main rotor hub Doppler frequency was constrained to less than 25 kHz, consistent with its diameter;

- only the front edge of the main rotor was visible with a Doppler frequency consistent with its diameter; and

- both the positive and negative Doppler frequencies of the tail rotor were visible only at several aspect angles.

In conclusion, we have presented and analyzed Doppler signature data for a hovering Hind-D helicopter. The Doppler signature was shown to be consistent with predictions based on the size, shape, and rotating velocities of the various moving parts. The measurements were limited to a small set of possible aspect angles. To fully characterize the helicopter signature for use in simulating a different encounter geometry, a more comprehensive set of measurements is needed. These additional measurements would include more depression angles and a detailed look at the main rotor hub Doppler signature, which has a great deal of fine detail.

Distribution

Admnstr
Defns Techl Info Ctr
Attn DTIC-OCP
8725 John J Kingman Rd Ste 0944
FT Belvoir VA 22060-6218

Under Secy of Defns for Rsrch & Engrg
Attn Rsrch & Advncd Techlgy
Depart of Defns
Washington DC 20301

NGIC
Attn Iang RSC S Carter
Charlottesville VA 22902-5396

US Army Armament RDE Ctr
Attn SMCAR-FSP-A1 M Rosenbluth
Attn SMCAR-FSP-A1 R Collett
Picatinny Arsenal NJ 07806-5000

US Army Missile Lab
Attn AMSMI-RD Advanced Sensors Dir
Attn AMSMI-RD Sys Simulation & Dev Dir
Attn AMSMI-RD-AS-MM G Emmons
Attn AMSMI-RD-AS-MM M Christian
Attn AMSMI-RD-AS-MM M Mullins
Attn AMSMI-RD-AS-RPR Redstone Sci Info
  Ctr
Attn AMSMI-RD-AS-RPT Techl Info Div
Attn AMSMI-RD-SS-HW S Mobley
Redstone Arsenal AL 35809

US Army Rsrch Ofc
Attn B D Guenther
Attn C Church
PO Box 12211
Research Triangle Park NC 27709-2211

Nav Rsrch Lab
Attn 2600 Techl Info Div
4555 Overlook Ave SW
Washington DC 20375

Nav Surface Weapons Ctr
Attn DX-21 Library Div
Dahlgren VA 22448

Nav Weapons Ctr
Attn 38 Rsrch Dept
Attn 381 Physics Div
China Lake CA 93555

Georgia Institite of Techlgy Georgia Tech
  Rsrch Inst
Attn Radar & Instrmntn Lab R McMillan
Attn Radar & Instrmntn Lab T L Lane
Atlanta GA 30332

VA Polytechnic Inst & State Univ
  Elect Interaction Lab
Attn G S Brown
Bradley Dept of Elect Engrg
Blacksburg VA 24061-0111

Eviron Rsrch Inst of MI
Attn IRIA Lib
PO Box 134001
Ann Arbor MI 48113-4001

US Army Rsrch Lab
Attn AMSRL-SE-RM B Bender
Attn AMSRL-SE-RM S Stratton
Aberdeen Proving Ground MD 21005

US Army Rsrch Lab
Attn AMSRL-CI-LL Techl Lib (3 copies)
Attn AMSRL-CS-AL-TA Mail & Records
  Mgmt
Attn AMSRL-CS-EA-TP Techl Pub (3 copies)
Attn AMSRL-SE J M Miller
Attn AMSRL-SE J Pellegrino
Attn AMSRL-SE-R B Wallace
Attn AMSRL-SE-RM D Hutchins
Attn AMSRL-SE-RM D Wikner
Attn AMSRL-SE-RM E Burke

Distribution (cont'd)

US Army Rsrch Lab (cont'd)
Attn AMSRL-SE-RM G Goldman
Attn AMSRL-SE-RM H Dropkin
Attn AMSRL-SE-RM J Nemarich
Attn AMSRL-SE-RM J Silverstein
Attn AMSRL-SE-RM J Silvious (10 copies)
Attn AMSRL-SE-RM R Dahlstrom
Attn AMSRL-SE-RM R Wellman (20 copies)
Attn AMSRL-SE-RU B Scheiner
Attn AMSRL-SE-RU J Sichina
Attn AMSRL-SE-SR D Rodkey
Adelphi MD 20783-1197

REPORT DOCUMENTATION PAGE

Public reporting burden for this collection of information is estimated to average 1 hour per response, including the time for reviewing instructions, searching existing data sources, gathering and maintaining the data needed, and completing and reviewing the collection of information. Send comments regarding this burden estimate or any other aspect of this collection of information, including suggestions for reducing this burden, to Washington Headquarters Services, Directorate for Information Operations and Reports, 1215 Jefferson Davis Highway, Suite 1204, Arlington, VA 22202-4302, and to the Office of Management and Budget, Paperwork Reduction Project (0704-0188), Washington, DC 20503.

1. AGENCY USE ONLY *(Leave blank)*	2. REPORT DATE July 1998	3. REPORT TYPE AND DATES COVERED Final, from May 1996 to July 1996

4. TITLE AND SUBTITLE Doppler Signature Measurements of an Mi-24 Hind-D Helicopter at 92 GHz	5. FUNDING NUMBERS PE: P62120A
6. AUTHOR(S) Ronald J. Wellman and Jerry L. Silvious	

7. PERFORMING ORGANIZATION NAME(S) AND ADDRESS(ES) U.S. Army Research Laboratory Attn: AMSRL-SE-RM (rwellman@arl.mil) 2800 Powder Mill Road Adelphi, MD 20783-1197	8. PERFORMING ORGANIZATION REPORT NUMBER ARL-TR-1637
9. SPONSORING/MONITORING AGENCY NAME(S) AND ADDRESS(ES) U.S. Army Research Laboratory 2800 Powder Mill Road Adelphi, MD 20783-1197	10. SPONSORING/MONITORING AGENCY REPORT NUMBER

11. SUPPLEMENTARY NOTES

ARL PR: 6N6360
AMS Code: 622120.H16

12a. DISTRIBUTION/AVAILABILITY STATEMENT Approved for public release; distribution unlimited.	12b. DISTRIBUTION CODE

13. ABSTRACT *(Maximum 200 words)*

This report describes millimeter wave Doppler signature measurements made on a hovering Mi-24 Hind-D helicopter. The measurement system, a CW sensor operating at 92 GHz, is described in detail. The recording system consisted of a high speed A/D board installed in a dual Pentium computer running Windows NT. The report presents the results of the Doppler analysis of the data. The signatures created by the rotating blades of the jet turbines known as jet engine modulation (JEM) lines and the Doppler signature components created by the many moving parts of the main and tail rotor assemblies are discussed in detail and a comparison to the theoretical values is presented.

14. SUBJECT TERMS Doppler, MMW, signature			15. NUMBER OF PAGES 21
			16. PRICE CODE

17. SECURITY CLASSIFICATION OF REPORT Unclassified	18. SECURITY CLASSIFICATION OF THIS PAGE Unclassified	19. SECURITY CLASSIFICATION OF ABSTRACT Unclassified	20. LIMITATION OF ABSTRACT UL

NSN 7540-01-280-5500

Standard Form 298 (Rev. 2-89)
Prescribed by ANSI Std. Z39-18
298-102